

Bandwidth of Step-Index Fibers with Microbending

by Michel Clapeau* and Jacques Arnaud*

The steady-state microbending loss of step-index multimode fibers is found to be, within the WKB approximation, $6.27 (\gamma/\Delta)$ dB/unit length, where γ denotes the spectral density of the curvature process. The product of the square of the pulse broadening improvement factor \mathcal{R} and loss \mathcal{L} is 0.74 dB. Results are given for various excitation conditions.

Bandbreite von Stufenprofilfasern mit Mikrokrümmungen

Die stationären Mikrokrümmungsverluste von Stufenprofilfasern ergeben sich im Rahmen der WKB-Näherung zu $6.27 (\gamma/\Delta)$ dB/Länge, mit γ als spektraler Dichte der Krümmungsverteilung. Das Produkt aus Dämpfung und Verbesserungsfaktor zum Quadrat für die Impulsaufweitung ist 0,74 dB. Die Theorie wird für verschiedene Anregungsbedingungen ausgewertet.

There is a distinct possibility that the bandwidth of multimode fibers, particularly step-index fibers, can be drastically increased by random deformations. Marcuse [1] has shown that the product of the square of the pulse-broadening improvement factor \mathcal{R} and the excess loss \mathcal{L} is independent of the distortion strength. This product, however, depends on the index profile (e.g., step-index or square-law), the type of deformation (e.g., core diameter variations or microbending) and the spectrum of the deformation (e.g., uniform, peaked, or rapidly decreasing). It is not known yet how low the product $\mathcal{R}^2\mathcal{L}$ can be, because the limitations that fabrication techniques impose on the distortion spectra have not been sufficiently investigated and also because previous theories are somewhat inaccurate.

The first detailed expressions for the effect of random distortion on the fiber bandwidth were obtained from coupled-mode theory taken to the limit of continuous mode numbers [1]. It now appears that rigorously equivalent results can be obtained from ray theory: The rate of pulse broadening can be obtained by integrating time along the ray trajectories [2] and the impulse response can be shown to be gaussian for large lengths as a consequence of the central limit theorem.

In modal theories, a number of approximations were made (use of principal mode number, neglect of the coupling between nonadjacent modes) that are open to question [3]. In contradistinction, the ray theories presented in [3] and [4] are rigorous (within the WKB approximation) and applicable to any index profile and any curvature spectrum. In the present paper we shall only consider for clarity lossless step-index fibers and uniform curvature spectra. We discuss both the irradiance patterns and the fiber bandwidth. For large distances, the approximate results of Olshansky [5] turn out to be quite accurate. However, for non-uniform spectra, the two-dimensional results in [6]

indicate that the approximations used in [5] may lead to large errors.

In the following, the core radius is denoted r_c , the relative index step Δ , and the group velocity in the core material $u_0 \approx c/n_0$, if n_0 denotes the core index. The fiber axis has local curvatures $C_x(z)$ and $C_y(z)$ in the x, z - and y, z -planes respectively, z being a coordinate along the fiber axis. We assume that the spectral densities of these curvature processes

$$G_{x,y}(\Omega) = \int_{-\infty}^{+\infty} \langle C_{x,y}(z) C_{x,y}(z+\zeta) \rangle \exp(i\Omega\zeta) d\zeta \quad (1)$$

assume a constant value γ , and that C_x, C_y are uncorrelated. A mode of propagation can be specified by its normalized propagation constant $\varepsilon = (\theta/\theta_c)^2$ with $0 < \varepsilon < 1$ and azimuthal mode number ν . The value $\nu=0$ corresponds to meridional rays and $\varepsilon = \nu^2$ to helical rays. Thus the admissible region in the ε, ν -plane is shown in Fig. 1. If we neglect the transmission of rays such that $\varepsilon > 1$ (or $\theta > \theta_c$), we must impose on the optical power $P^\dagger(\varepsilon, \nu, z)$ the condition $P^\dagger(1, \nu, z) = 0$. For step-index fibers, we set $\tilde{U}=0$ in eq. (8) of [4]. We can evaluate explicitly the average radius squared R . In normalized quantities, we have

$$\frac{\partial P^\dagger}{\partial z} = \frac{\partial P^\dagger}{\partial \varepsilon} + \varepsilon \frac{\partial^2 P^\dagger}{\partial \varepsilon^2} + \frac{1}{12} \left(1 + 2 \frac{\nu^2}{\varepsilon} \right) \frac{\partial^2 P^\dagger}{\partial \nu^2} + \nu \frac{\partial^2 P^\dagger}{\partial \varepsilon \partial \nu} \quad (2)$$

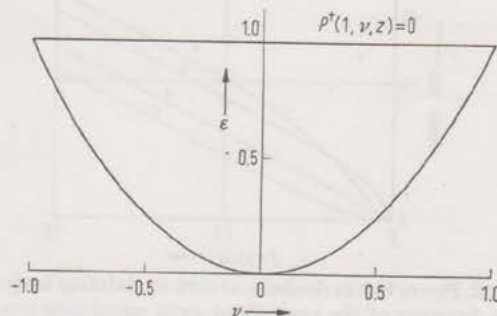


Fig. 1. Domain of integration of the Fokker-Planck equation in the ε, ν -plane. P^\dagger is required to vanish for $\varepsilon = 1$ ($\theta = \theta_c$).

* Dr. M. Clapeau, Prof. Dr. J. Arnaud, Laboratoire d'Électronique des Microondes, UER des Sciences, 123 rue A. Thomas, F-87060 Limoges Cedex, France.

where $\bar{z} \equiv \gamma z/\Delta$. This equation is solved numerically from some initial distribution $P^\dagger(\varepsilon, \nu, 0)$ by a straightforward procedure along the z -axis. The z -increment is small enough to avoid numerical instabilities. The number of points in the ε, ν -plane is about 1250. A full solution of eq. (2) requires only 15 minutes on a MITTRA 15 computer. The total power for some fiber length $z = L$ is obtained by integrating over ε and ν in the area shown in Fig. 1 the quantity $P(\varepsilon, \nu, z) = Z_n(\varepsilon, \nu) P^\dagger(\varepsilon, \nu, z)$ where the normalized ray period Z_n is given by

$$Z_n(\varepsilon, \nu) = (\varepsilon - \nu^2)^{1/2}/\varepsilon. \quad (3)$$

The statistical modes are obtained by setting $\partial/\partial z = -\lambda z$ in eq. (2), where λ represents the microbending loss. For the statistical modes such that P^\dagger is independent of ν , the analytic solution of eq. (2) is

$$P_m(\varepsilon, \nu, z) = Z_n(\varepsilon, \nu) J_0(u_{0m} \sqrt{\varepsilon}) \quad (4)$$

where u_{0m} is the m th zero of the Bessel function $J_0(\cdot)$. The corresponding losses are

$$\begin{aligned} \alpha_0 &= 6.27 \gamma/\Delta, & \alpha_1 &= 33.06 \gamma/\Delta, \\ \alpha_2 &= 81.25 \gamma/\Delta \end{aligned} \quad (5)$$

decibels per unit length. The far-field pattern is (leaving aside the refraction at the fiber tip)

$$I_m(\theta) = J_0(u_{0m} \theta/\theta_c) \quad (6)$$

and the near-field intensity is

$$I'_m(r) = E(\pi/2, r/r_c) \quad (7)$$

where $E(\cdot, \cdot)$ denotes an elliptic integral of the second kind.

Numerically, we have verified the analytical result in eq. (4), and we have investigated the evolution of the microbending loss as a function of the fiber length for various excitation conditions (see Fig. 2). We verify in Fig. 2 that the slope of the curves for large z is that given by α_0 in eq. (5) independently of the excitation conditions. But for many short fibers, the large z behaviour may not be reached, and therefore our numerical results are needed.

To investigate the bandwidth of the fiber we need augment the left-hand side of eq. (2) by a term $(\Delta^2/\gamma u_0) \varepsilon \partial P^\dagger/\partial t$ and Fourier transform $P(t)$ into $\tilde{P}(\Omega)$, where Ω denotes the baseband angular frequency.

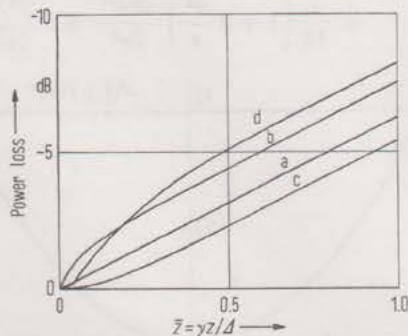


Fig. 2. Power loss in decibels, at zero modulation frequency, as a function of the normalized axial coordinate $\bar{z} = \gamma z/\Delta$ for various excitation conditions; (a) steady-state distribution, (b) $P(\varepsilon, \nu, 0) = \delta(\nu)$, (c) $\delta(\nu)$ ($\varepsilon \leq 1/2$), (d) $\delta(\nu) \cdot \delta(\varepsilon - 1/2)$, where δ denotes Dirac's function.

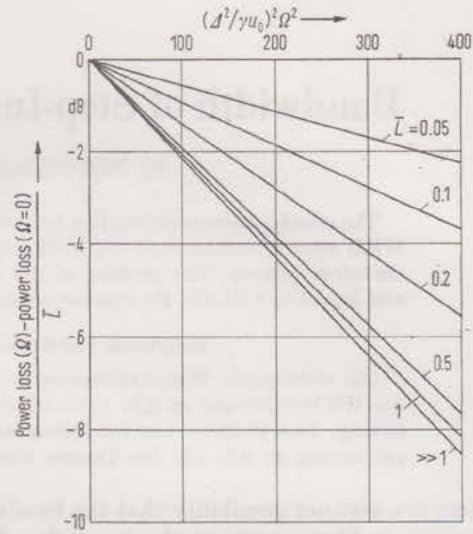


Fig. 3. Normalized power loss in decibels as a function of the normalized modulation angular frequency $(\Delta^2/\gamma u_0)^2 \Omega^2$ for various normalized fiber lengths $\bar{L} = \gamma L/\Delta$.

quency. For numerical purposes, we set $\tilde{P} = \tilde{R} + i\tilde{I}$, and solve the corresponding pair of equations for \tilde{R} and \tilde{I} by the same straightforward numerical procedure used for P . We have plotted in Fig. 3 the power loss $10 \log_{10}(\tilde{R}^2 + \tilde{I}^2)^{1/2}$ as a function of Ω^2 , for various fiber lengths L and for a Lambertian excitation. (\tilde{R} and \tilde{I} denote integrals of \tilde{R} and \tilde{I} , respectively, over ε and ν .) When $\bar{L} = \gamma L/\Delta \gg 1$ the impulse (and frequency) response is gaussian and thus the curve is a straight line. We find from the slope of that straight line

$$\mathcal{R}^2 \mathcal{L} = 0.74 \text{ dB}; \quad \bar{L} \gg 1 \quad (8)$$

where \mathcal{L} denotes the steady-state microbending loss and $\mathcal{R}^2 \equiv \sigma^2/\sigma_0^2$ denotes the square of the impulse width, with (σ) and without (σ_0) distortion. It turns out that those values for α_0 and $\mathcal{R}^2 \mathcal{L}$ are within a few per cent of the values given by Olshansky [5]. But we do not expect this agreement with approximate modal theories to be maintained for peaked or otherwise distorted curvature spectra.

(Received May 31st, 1979.)

References

- [1] Marcuse, D., Theory of dielectric optical waveguides. Academic Press, New York 1974.
- [2] Rousseau, M. and Arnaud, J., Ray theory of the impulse response of randomly bent multimode fibers. J. Opt. Quantum Electron. 10 [1978], 53–59.
- [3] Arnaud, J., Use of principal mode numbers in the theory of microbending. Electron. Letters 14 [1978], 663–664.
- [4] Arnaud, J. and Rousseau, M., Ray theory of randomly bent multimode optical fibers. Opt. Letters 3 [1978], 63–65.
- [5] Olshansky, R., Mode coupling effects in graded index optical fibers. Appl. Opt. 14 [1975], 935–945.
- [6] de Fornel, F., Role of Nonadjacent mode coupling in the theory of microbending. Opt. Commun. 28 [1979], 55–58.